Influence of Nb Doping on Magnetic Properties of Nanocrystalline Nd-Fe-B Alloys

V. Bilovol[1], S. Ferrari[1], L. G. Pampillo[1], D. Derewnicka[2], M. Spyra[3], and F. D. Saccone[1]

[1]Instituto de Tecnología y Ciencias de la Ingeniería "Ing. Hilario Fernández Long," UBA-CONICET, Ciudad Autónoma de Buenos Aires, Argentina

[2]Institute of Precision Mechanics, Warsaw 01-796, Poland

[3]Faculty of Materials Science and Engineering, Warsaw University of Technology, Warsaw 02-507, Poland

The influence of Nb doping was studied on ribbons of nominal composition $Nd_yFe_{86-x-y}B_{14}Nb_x$ $(y = 7, 8;\ x = 0, 2, 4)$. The alloys were prepared by melt-spinning and then annealed at 973 K for 20 minutes. The magnetic characterization revealed that niobium addition improves substantially the magnetic properties of the studied alloys. The structural characterization showed that, in most alloys, the magnetically hard phase $Nd_2Fe_{14}B$ precipitated as the main phase. This was not the case for the ternaries $(x = 0)$ and for the $Nd_7Fe_{77}B_{14}Nb_2$ alloys. Furthermore, the addition of Nb inhibited the precipitation of α-Fe, independently of the Nd content. From the complete set of samples studied in this work, we found that the sample with nominal composition $Nd_8Fe_{74}B_{14}Nb_4$ exhibited the highest coercive field $H_C = 575$ kA/m while $Nd_7Fe_{75}B_{14}Nb_4$ showed the highest maximum energy product, $(BH)_{max} = 73$ kJ/m^3.

***Index Terms*—Doping, magnetic properties, nanocomposites.**

I. Introduction

NEODYMIUM-IRON-BORON nanocomposite permanent magnets were developed in the early 1990s [1], [2]. Their low neodymium content, less than the stoichiometric amount of 12% at., made them cheaper and more corrosion resistant. In addition, the increased boron content improves the tendency to amorphization. These systems, called exchange—spring magnets, exhibit interesting magnetic properties due to exchange coupling between hard and soft magnetic phases at nanometric scale. The coexistence of both type of magnetic phases enhances the remanence and the magnetic energy product. However, the presence of the soft phases reduces the coercivity. The addition of alloying components such as Mn, Cu, Nb, Ti, Mo, etc. helps to control the grain growth during melt—spinning production of magnets of this kind and also improves their magnetic response [3]–[8]. In particular, the addition of Nb was reported to be very effective in promoting grain refinement of nanocomposites, leading to improved coercivity [9]. However, the mechanisms that originate the suppression of α-Fe formation as well as the role of Nb as an additive which helps to stabilize the $Nd_2Fe_{14}B$ phase are not fully understood.

The purpose of the present work is to investigate the influence of niobium doping on the magnetic properties and phase constitution of NdFeB systems produced by the melt spinning technique and subsequently annealed.

II. Experimental

$Nd_yFe_{(86-x-y)}B_{14}Nb_x$ $(y = 7, 8; x = 0, 2, 4)$ rapidly quenched ribbons obtained by melt-spinning with the roll speed of 30 m/s were annealed for 20 min at 973 K. Magnetic properties were measured using a LakeShore 7404 vibrating sample magnetometer with a maximum applied field of 1.9 T. Detailed information on the phase constitution was obtained from Mössbauer spectroscopy as well as by X-ray diffraction (XRD). The Mössbauer measurements were recorded at room temperature (RT) under transmission geometry with a standard constant acceleration spectrometer, using a 5 mCi ^{57}CoRh radioactive source. Data was recorded using a 1024 channel MDAQ107 data acquisition module [10]. The isomer shifts δ were referred to RT α-Fe. Amorphous and crystalline ribbons were characterized by X-ray diffraction in a $\theta - 2\theta$ diffractometer (Rigaku D/max equipped with a horizontal goniometer), using Cu-Kα radiation. The microstructure of alloys was observed on high-resolution transmission electron microscope (FEI TITAN CUBED 80–300). From here the samples will be named as Nd_yNb_x $(y = 7, 8; x = 0, 2, 4)$.

TABLE I
Magnetic Properties of Annealed Samples
(Typical Error Less Than 3%)

	$_JH_c$ [kA/m]	M_r [kA/m]	M_r/M_s	$(BH)_{max}$ [kJ/m^3]
Nd8Nb4	575	515	0.84	66.4
Nd8Nb2	473	596	0.70	61.1
Nd8Nb0	105	342	0.43	10.0
Nd7Nb4	453	615	0.83	73.0
Nd7Nb2	83.5	715	0.65	18.7
Nd7Nb0	25	357	0.33	2.7

III. Results and Discussion

Magnetic measurements performed on ribbons, with typical sizes 1 mm wide and 5 mm length, revealed that the addition of a small percent of Nb to the ternary alloy improves their magnetic performance (see Table I). All the values reported there, were fitted employing a proposed function [11] for the descending branch of the hysteresis loop.

Among all the samples studied in this work, it was found that the alloy with nominal composition $Nd_7Fe_{75}B_{14}Nb_4$ (Nd7Nb4 sample) exhibited the highest maximum energy

Manuscript received February 16, 2013; revised March 28, 2013; accepted April 05, 2013. Date of current version July 23, 2013. Corresponding author: L. G. Pampillo (e-mail: lpampillo@fi.uba.ar).

Color versions of one or more of the figures in this paper are available online at http://ieeexplore.ieee.org.

Digital Object Identifier 10.1109/TMAG.2013.2257707

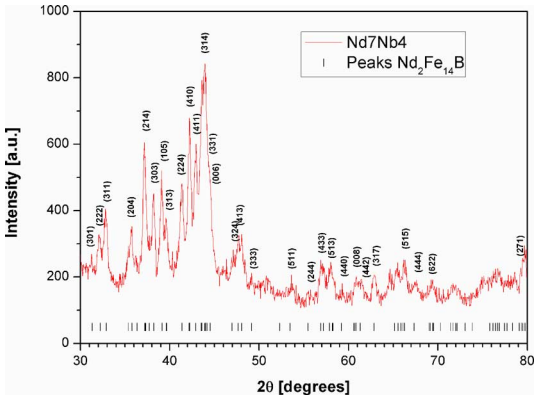

Fig. 1. Diffractogram corresponding to Nd7Nb4 (annealed sample). Indicated peaks correspond to $Nd_2Fe_{14}B$ phase. Miller indices of the most intense peaks are also marked.

TABLE II
CRYSTALLINE PHASES FOUND IN ANNEALED SAMPLES

Sample	Volume Percentages $Nd_2Fe_{14}B$	$Nd_2Fe_{23}B_3$	Others
Nd7Nb0	14.4 %	20.5 %	α-Fe, $Nd_{1.1}Fe_4B_4$, Fe_2B
Nd7Nb2	44.5 %	54.9 %	Fe_2B
Nd7Nb4	89.0 %	2.1 %	Fe_2B, $Fe_{23}B_6$
Nd8Nb0	33.7 %	13.9 %	α-Fe, $Nd_{1.1}Fe_4B_4$, Fe_2B
Nd8Nb2	97.5 %	2.1 %	Fe_2B
Nd8Nb4	95.1 %	3.6 %	Fe_2B

product, $(BH)_{max} = 73$ kJ/m^3 and $Nd_8Fe_{74}B_{14}Nb_4$ (Nd8Nb4 sample) the highest coercive field $H_C = 575$ kA/m.

In order to explain the magnetic improvement we also performed Mössbauer and XRD experiments to obtain information on the phase composition of the samples. The XRD patterns were fitted by Rietveld refinement using Maud program [12]. For example, Fig. 1 shows the diffractogram corresponding to Nd7Nb4 (annealed sample).

The amount in volume percentages of the dominant ternary crystalline phases found for each sample is reported in Table II. The results of the analysis are focused on the crystalline phases but the presence of the amorphous phase was not disregarded. The analysis of XRD patterns reveals that all samples contain the $Nd_2Fe_{14}B$ crystalline phase (magnetically hard) together with other expected phases such as $Nd_2Fe_{23}B_3$, $Nd_{1.1}Fe_4B_4$, Fe_2B and α-Fe. In ternary alloys α-Fe appears as the majority phase together with some amount of the $Nd_{1.1}Fe_4B_4$ phase. However, in the quaternary samples Fe_2B appears as a minority phase, while α-Fe is not present. The $Nd_2Fe_{23}B_3$ phase also appears in significant percentages but only in the ternaries and in the Nd7Nb2 sample ($Nd_7Fe_{77}B_{14}Nb_2$), which is the sample with the lowest amounts of Nd and Nb of all studied systems. This makes it clear that more Nd and a higher Nb doping fraction promote the growth and stabilization of the $Nd_2Fe_{14}B$ crystalline phase.

Mössbauer spectra of doped and annealed samples were fitted with six sextets (corresponding to 4e, 4c, $8j_1, 8j_2, 16k_1$ and $16k_2$, iron sites in $Nd_2Fe_{14}B$), one doublet (quadrupolar interaction corresponding to paramagnetic $Nd_{1.1}Fe_4B_4$) and a

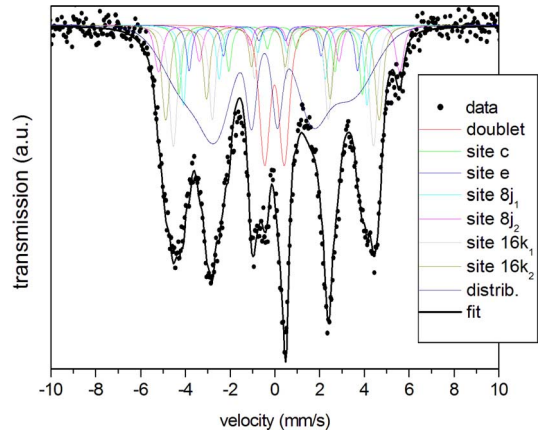

Fig. 2. Mössbauer spectrum of Nd7Nb4 (annealed sample).

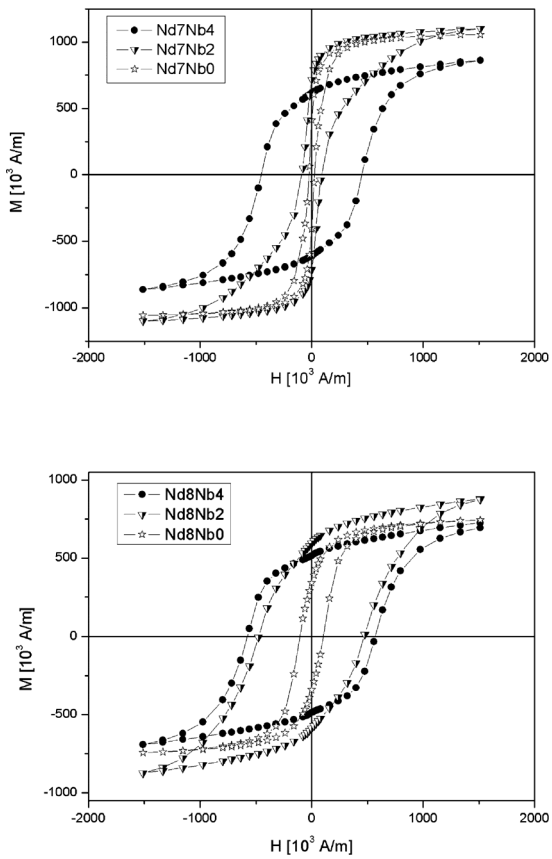

Fig. 3. Hysteresis loops corresponding to annealed samples: (Top) Nd7Nbx and (Bottom) Nd8Nbx (x = 0, 2, 4).

distribution of magnetic sextets (associated to an amorphous residual matrix). The fitted spectrum corresponding to Nd7Nb4 sample is shown in Fig. 2. It can be seen that a high fraction (30%–40%) of ^{57}Fe probes is present in the distribution of the magnetic sextets. This gives an indication of a large amount of the amorphous phase being present.

Fig. 3 shows hysteresis loops corresponding to all the studied annealed samples. Independently of the Nd percentages, alloys with Nb 4% at. have a lower saturation magnetization but a higher coercive fields which ultimately leads to a higher maximum energy product (see Table I).

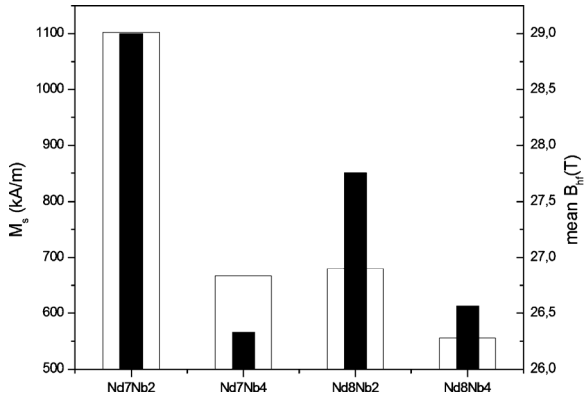

Fig. 4. Saturation magnetization (M_s) (black columns) and mean hyperfine field (mean B_{hf}) (white columns) as a function of Nd and Nb content.

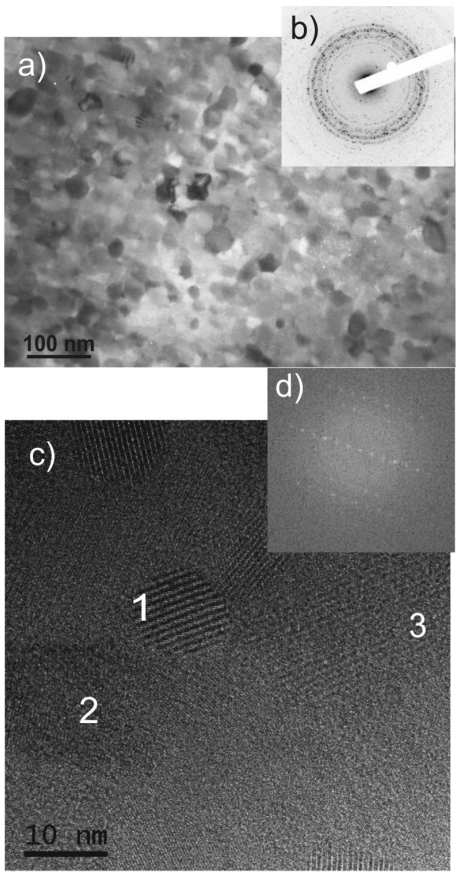

	Element [at.%]		
N°.analysis	Nd	Fe	Nb
1	12.7	84.9	2.4
2	10.4	83.0	6.6
3	7.6	87.9	4.5

Fig. 5. Structure of the annealed Nd8Nb4 alloy (a) TEM image; (b) an electron diffraction from the central area; (c) grains of $Nd_2Fe_{14}B$ in HR TEM mode; d) FET from the grain no. 3. Table shows chemical composition in the marked grains on Fig. 5(c).

Fig. 4 shows the values of saturation magnetization extracted from the hysteresis loops (left axis) and average hyperfine fields extracted from Mössbauer measurements (right axis). The latter values were calculated assuming a simple approximation model in which the magnetic moments of the main $Nd_2Fe_{14}B$ phase

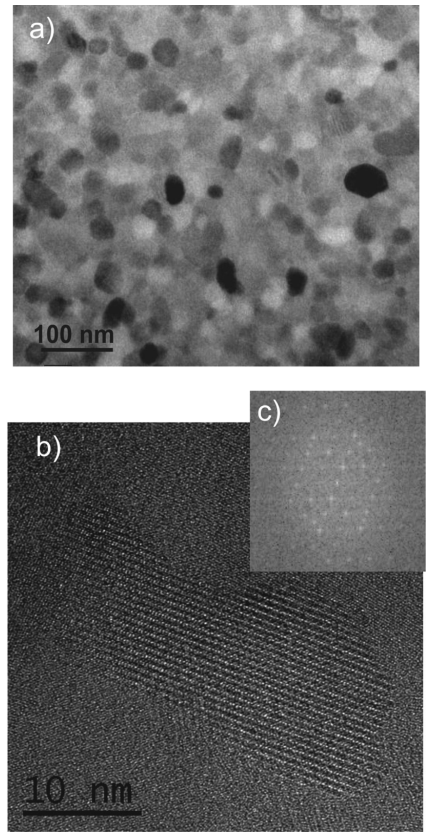

Fig. 6. Structure of the annealed Nd7Nb4 alloy (a) TEM image; (b) grains of $Nd_2Fe_{14}B$ in HR TEM mode; (c) the FET (TEM) from the grain in the centre.

are assumed to be parallel to those of the amorphous phase (magnetically soft) because of an exchange coupling existing between them. The values of hyperfine fields were simply averaged. It can be seen from a qualitative point of view that there is a clear correlation between both magnitudes as they both follow a very similar trend.

Fig. 5 shows the structure of the Nd8Nb4 alloy after annealing. The alloy contains grains with different size up to 50 nm [Fig. 5(a)]. Electron diffraction from this area shows not only the polycrystalline structure but also the amorphous halo. A closer look at the microstructure revealed small equiaxed grains [Fig. 5(c)]. The HR TEM image cannot distinguish the amorphous phase from unfavorably orientated grains. A FET image [Fig. 5(d)] obtained from the central grain confirms the presence of the $Nd_2Fe_{14}B$ grains. Point EDX analysis performed in the individual grains did not find any places free from the presence of Nb (see Table at the bottom of Fig. 5).

The structure of the annealed Nd7Nb4 alloy observed in Fig. 6 does not vary significantly from the Nd8Nb4 alloy. It contains slightly larger grains, up to 60 nm [Fig. 6(a)]. The grains are equiaxial and randomly oriented. HR TEM view confirms the presence of the $Nd_2Fe_{14}B$ phase [Fig. 6(b)].

The analysis of the obtained results indicates that addition of Nb retards nucleation and growth of α-Fe as well as contributes to the crystallization of the hard magnetic phase $Nd_2Fe_{14}B$ which is similar to the behavior of the Nd-Fe-B systems alloyed with other doping elements [13], [14]. The presence of the amorphous phase may influence the magnetic properties and

make them worse because of the unfavorable phase composition in the alloy. The precursor samples (before annealing) have crystalline phases embedded in an amorphous matrix. This amorphous phase could disappear at a higher annealing temperature, but this would result in the growth of larger grains, which is also not desirable in this type of materials.

IV. Conclusion

From the complete set of samples studied in this work we found that the sample with a nominal composition $Nd_8Fe_{74}B_{14}Nb_4$ exhibited the highest coercive field $H_C = 575$ kA/m while $Nd_7Fe_{75}B_{14}Nb_4$ showed the highest maximum energy product, $(BH)_{max} = 73$ kJ/m^3.

These properties are a result of a complementary contribution from the highly refined microstructure and a proper distribution of the soft and hard magnetic phases. The results indicate that incorporation of Nb retards nucleation and growth of α-Fe as well as contributes to crystallization of the hard magnetic phase $Nd_2Fe_{14}B$, similarly to what occurs in Nd-Fe-B systems modified with other doping elements such as titanium [14].

Acknowledgment

The authors acknowledge financial support from Argentine Agencies (CONICET and ANPCYT). Financial support from the Polish Ministry of Science and Higher Education (Grant Nr N 507 452834) is also gratefully acknowledged.

References

[1] R. Coehoorn, D. B. DeMooji, J. P. W. B. Duchateau, and K. H. J. Buschow, "Novel permanent magnetic materials made by rapid quenching," *J. Phys.*, vol. 49, pp. C8–669, 1988.

[2] E. Kneller and R. Hawig, "The exchange-spring magnet: A new material principle for permanent magnets," *IEEE Trans. Magn.*, vol. 27, pp. 3588–3600, 1991.

[3] S. Hirosawa, H. Kanekiyo, and M. Uehara, "High-coercivity iron-rich rare-earth permanent magnet material based on (Fe, Co)$_3$ B-Nd-M (M = Al, Si, Cu, Ga, Ag, Au)," *J. Appl. Phys.*, vol. 73, pp. 6488–6490, 1993.

[4] H. Kanekiyo, M. Uehara, and S. Hirosawa, "Microstructure and magnetic properties of high-remanence $Nd_5Fe_{71.5}$ $Co_5B_{18.5}$ M (M = Al, Si, Ga, Ag, Au) rapidly solidified and crystallized alloys for resin-bonded magnets," *IEEE Trans. Magn.*, vol. 29, pp. 2863–2865, 1993.

[5] S. Hirosawa and H. Kanekiyo, "Nanostructure and magnetic properties of chromium-doped Fe_3 B-$Nd_2Fe_{14}B$ exchange-coupled permanent magnets," *Mater. Sci. Eng. A*, vol. 217/218, pp. 367–370, 1996.

[6] M. Leonowicz, H. A. Davies, M. A. Al-Khafaji, T. Keates, and M. Crabbe, "Property enhancement for hot deformed Fe-Nd-B magnets by modification of composition of the Nd-rich phase," *IEEE Trans. Magn.*, vol. 30, pp. 651–653, 1994.

[7] R. Ishii, T. Miyoshi, H. Kaneniyo, and S. Hirosawa, "High-coercivity nanocomposite permanent magnet based on Nd-Fe-B-Ti-C with Cr addition for high-temperature applications," *J. Magn. Magn. Mat.*, vol. 312, pp. 410–413, 2007.

[8] I. Betancourt and H. A. Davies, "Enhanced coercivity in B-rich nanocomposite α-Fe/$(NdPr)_2Fe_{14}$ B/Fe_3B hard magnetic alloys," *Appl. Phys. Lett.*, vol. 87, p. 162516, 2005.

[9] I. Betancourt and H. A. Davies, "Magnetic properties of B-rich nanocomposite α-(Fe, Co)/$(NdPr)_2Fe_{14}B$ alloys," *Phys. B*, vol. 384, pp. 286–289, 2006.

[10] A. Veiga, M. A. Mayosky, N. Martínez, P. M. Zélis, G. A. Pasquevich, and F. H. Sánchez, "Smooth driving of Mössbauer electromechanical transducers," *Hyp. Inter.*, vol. 202, pp. 107–115, 2011.

[11] M. B. Stearns and Y. Cheng, "Determination of para and ferromagnetic components of magnetization and magnetoresistance of granular Co/Ag films," *J. Appl. Phys.*, vol. 75, p. 6894, 1994.

[12] L. Lutterotti, "Total pattern fitting for the combined size-strain-stress-texture determination in thin film diffraction," *Nuc. Inst. Meth. in Phys. Res. B*, vol. 268, pp. 334–340, 2010.

[13] M. Spyra, D. Derewnicka, and M. Leonowicz, "Lean neodymium Nd-Fe-B magnets containing minor addition of titanium," *Phys. Stat. Solidi A*, vol. 207, pp. 1170–1173, 2010.

[14] M. K. Leonowicz, M. Spyra, B. Michalski, W. Kaszuwara, and D. Derewnicka, "Effect of composition and structure on the properties of Ti containing Nd-Fe-B rapidly quenched alloys," *IEEE Trans. Magn*, vol. 48, pp. 3150–3153, 2012.